

## Supporting information

### **Buried Interface Management toward High-Performance Perovskite Solar Cells†**

Bin Du<sup>a##</sup>, Yuexin Lin<sup>b#</sup>, Jintao Ma<sup>a</sup>, Weidan Gu<sup>a</sup>, Fei Liu<sup>a</sup>, Yijun Yao<sup>c\*</sup>, and Lin Song<sup>d\*</sup>

<sup>a</sup> *School of Materials Science and Engineering, Xi'an Polytechnic University, Xi'an 710048, China*

<sup>b</sup> *MOE Key Laboratory for Nonequilibrium Synthesis and Modulation of Condensed Matter, School of Physics, National Innovation Platform (Center) for Industry-Education Integration of Energy Storage Technology, Xi'an Jiaotong University, Xi'an 710049, P. R. China*

<sup>c</sup> *School of Textile Science and Engineering, Xi'an Polytechnic University, Xi'an, 710048, Shaanxi, China*

<sup>d</sup> *Frontiers Science Center for Flexible Electronics (FSCFE), Institute of Flexible Electronics (IFE), Northwestern Polytechnical University, Xi'an 710072, China*

# Authors share equal authorship

† Electronic supplementary information (ESI) available.

\* [dubin@xpu.edu.cn](mailto:dubin@xpu.edu.cn) (B. D)

\* [yaoyj@xpu.edu.cn](mailto:yaoyj@xpu.edu.cn) (Y. Y)

\* [iamsong@nwpu.edu.cn](mailto:iamsong@nwpu.edu.cn) (L. S)

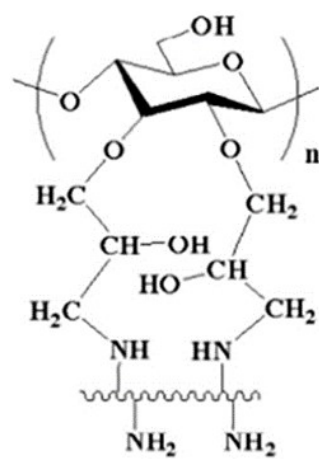


**Fig. S1.** Structure diagram of the molecular formula of GCC.

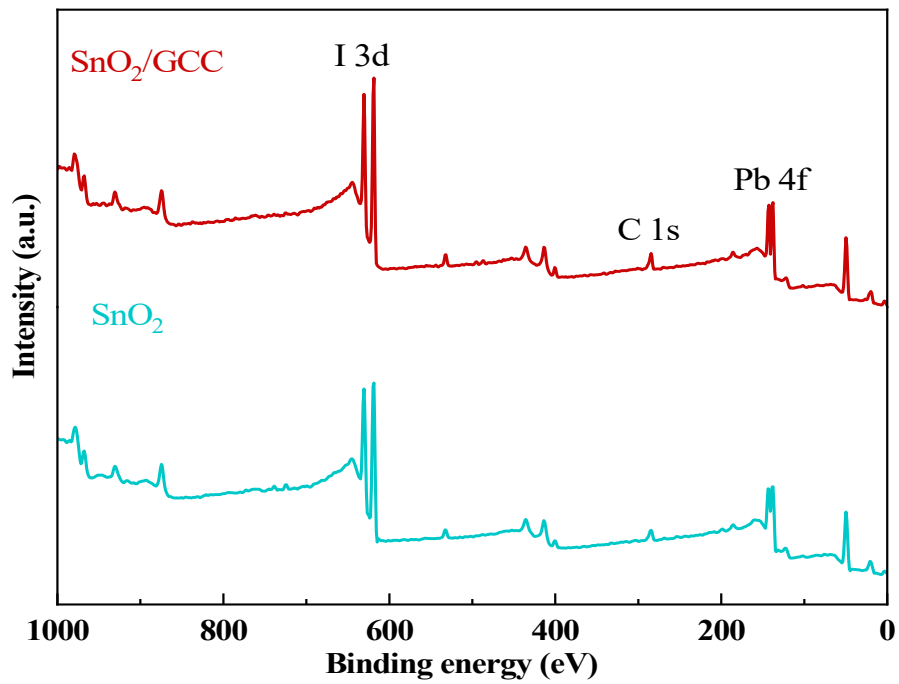


**Fig. S2.** XPS full spectra of  $\text{SnO}_2$  and  $\text{SnO}_2/\text{GCC}$ .

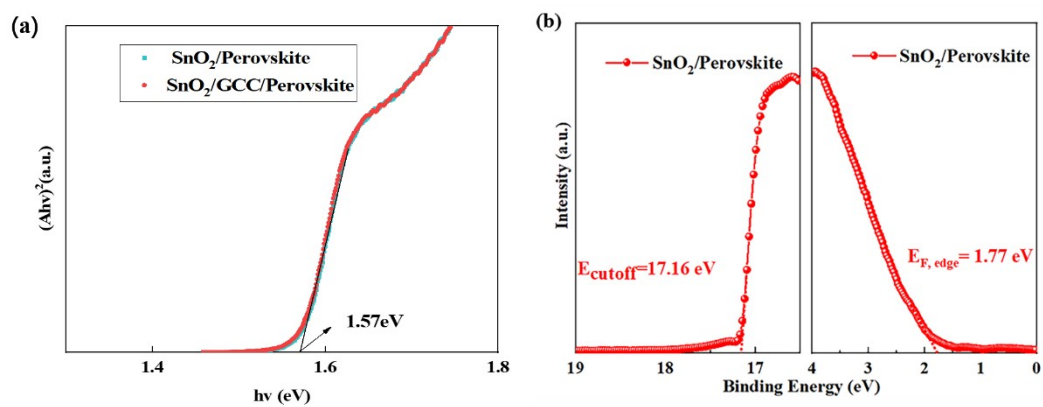


**Fig. S3.** (a) Tauc-Plot spectrum of perovskite films deposited on  $\text{SnO}_2/\text{Perovskite}$  substrate. (b) UPS spectra of  $\text{SnO}_2/\text{Perovskite}$  film.

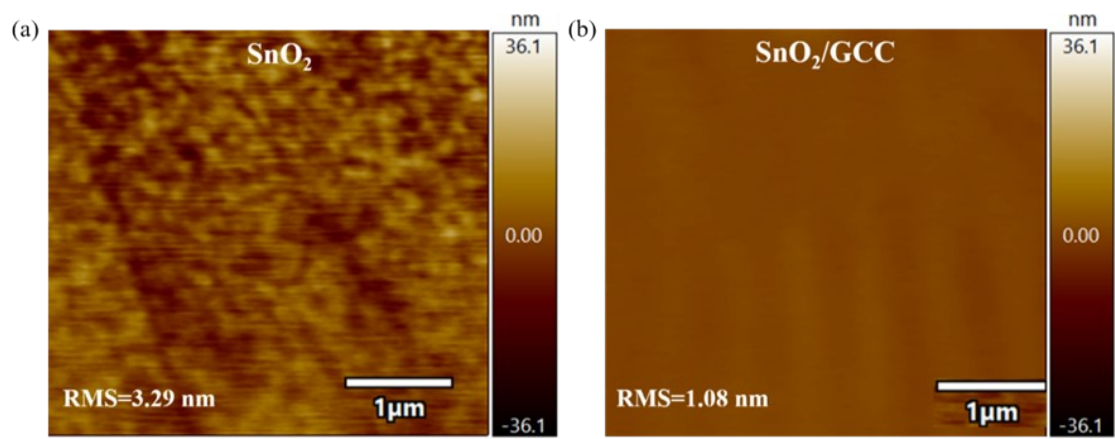


**Fig. S4.** AFM images of (a) SnO<sub>2</sub> and (b) SnO<sub>2</sub>/GCC films.

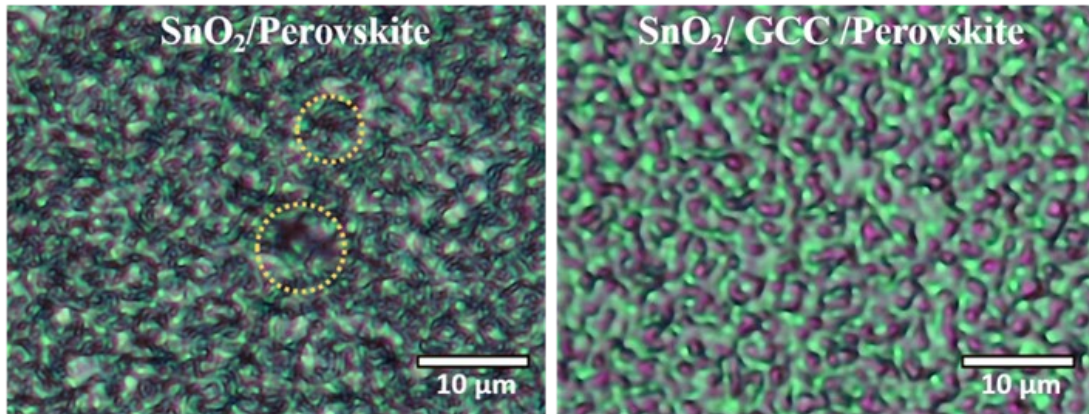


**Fig. S5.** OM images of perovskite films deposited on (a) SnO<sub>2</sub> and (b) SnO<sub>2</sub>/GCC ETLs.

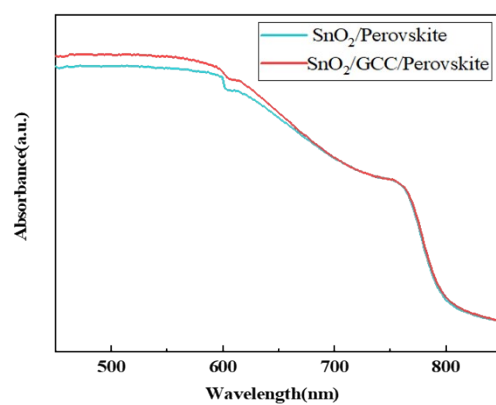


**Fig. S6.** UV-vis absorption spectra of perovskite films deposited on SnO<sub>2</sub> and SnO<sub>2</sub>/GCC ETLs.

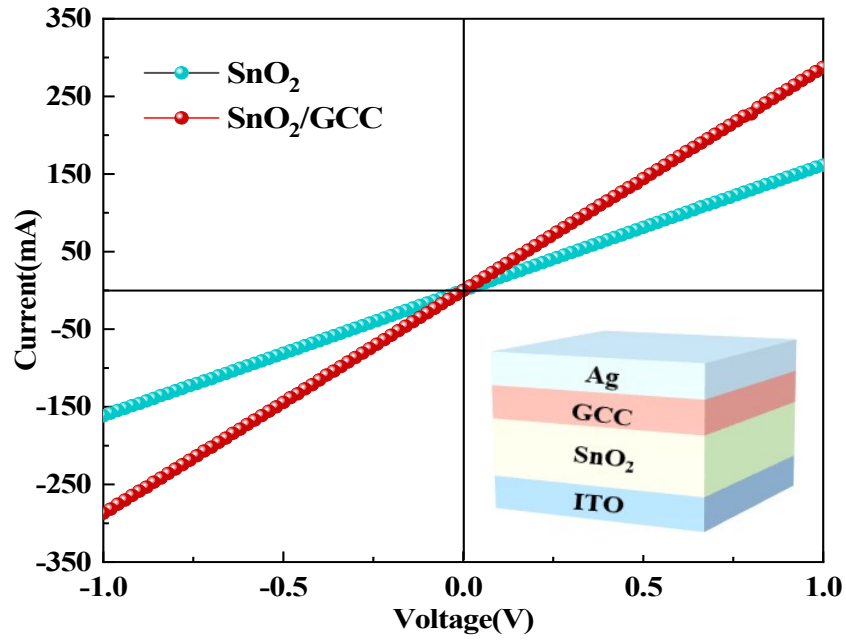


**Fig. S7.**  $I-V$  curves of devices based on  $\text{SnO}_2$  and  $\text{SnO}_2/\text{GCC}$  ETLs. The inset depicts the device structure.



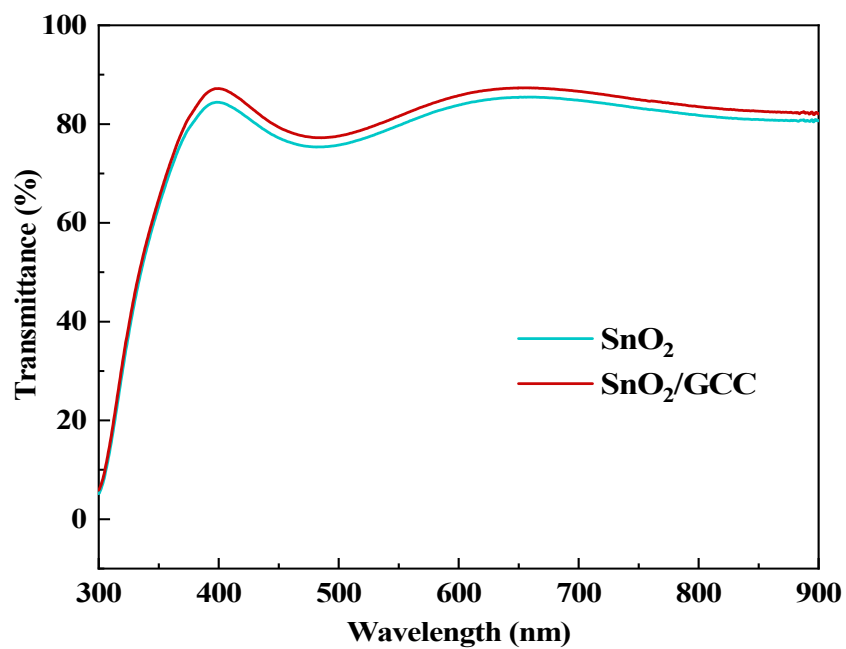


**Fig. S8.** UV-vis absorption spectra of SnO<sub>2</sub> and SnO<sub>2</sub>/GCC ETLs.

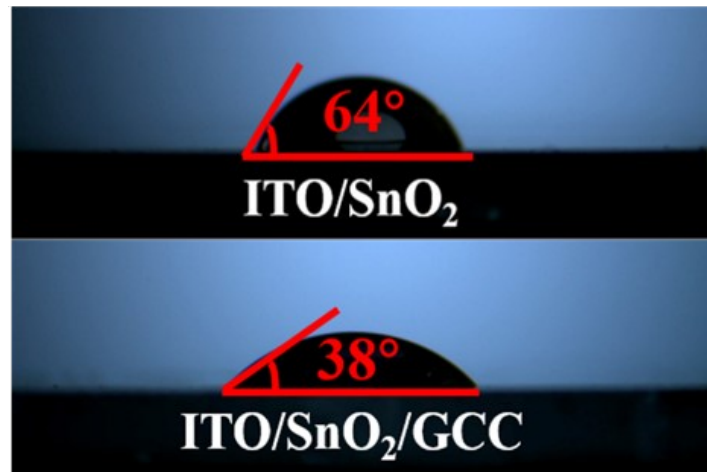


**Fig. S9.** The contact angle measurements of ITO/SnO<sub>2</sub> and ITO/SnO<sub>2</sub>/GCC ETLs.

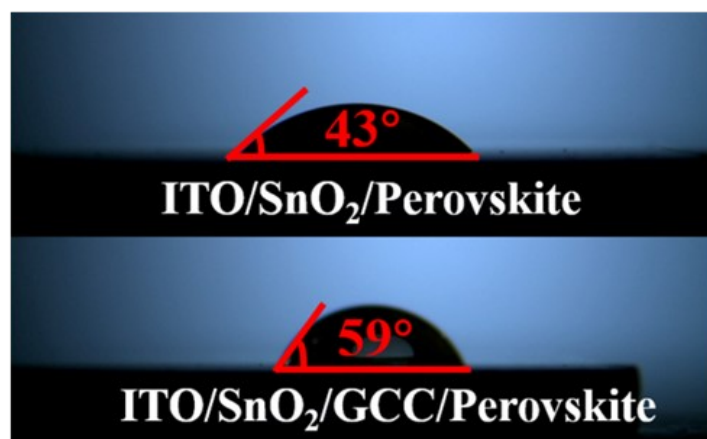


**Fig. S10.** The contact angle measurements of perovskite precursor solution on ITO/SnO<sub>2</sub> and ITO/SnO<sub>2</sub>/GCC.

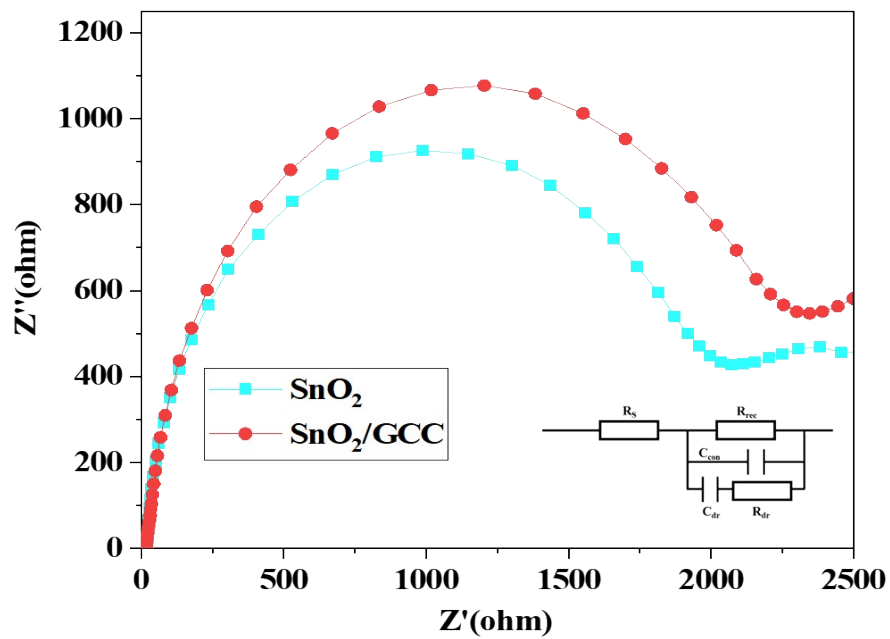


**Fig. S11.** Electrochemical impedance spectroscopy (EIS) at a bias of 0.9 V under dark conditions.

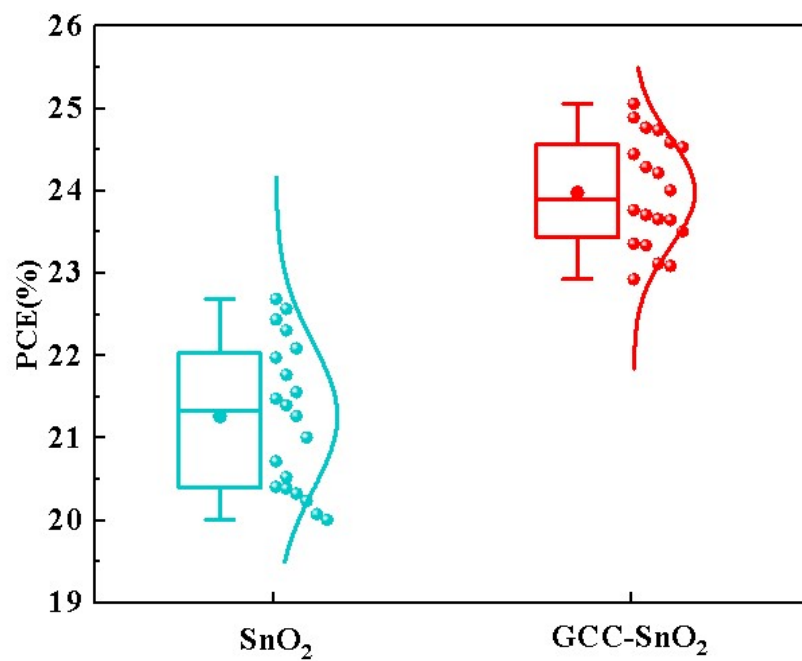


**Fig. S12.** PCE statistical data of SnO<sub>2</sub> and GCC-SnO<sub>2</sub>.

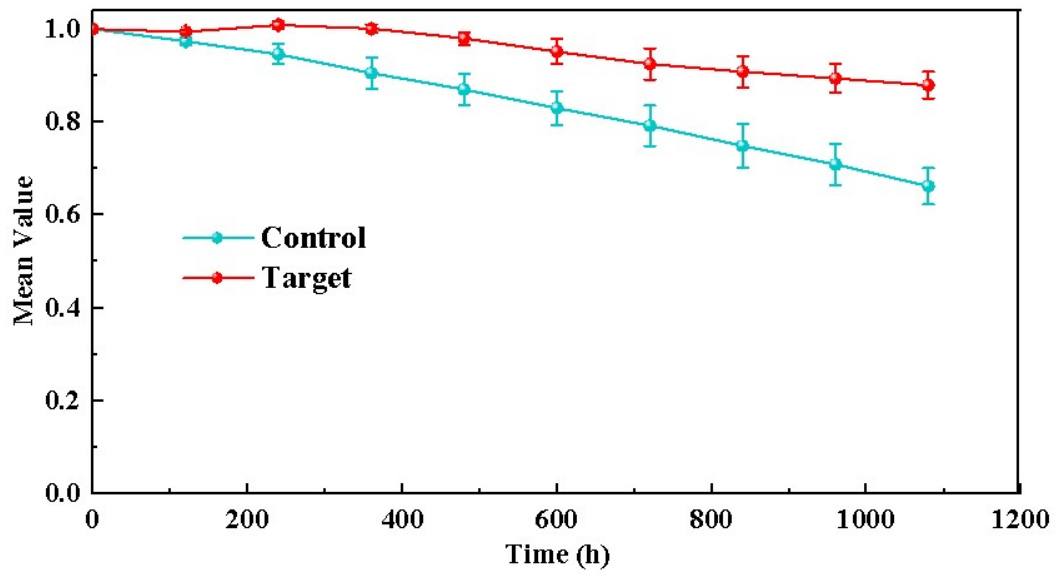


**Fig. S13.** Long term stability of unencapsulated PSC manufactured on raw and GCC modified SnO<sub>2</sub> measured in ambient air after 1200 hours.

**Table S1.** Calculated parameters for the energy level of SnO<sub>2</sub> and SnO<sub>2</sub>/GCC.

<b>Sample</b>	<b>E<sub>cutoff</sub> (eV)</b>	<b>W<sub>F</sub> (eV)</b>	<b>E<sub>F, edge</sub> (eV)</b>	<b>E<sub>VB</sub> (eV)</b>	<b>E<sub>g</sub> (eV)</b>	<b>E<sub>CB</sub> (eV)</b>
<b>SnO<sub>2</sub></b>	<b>16.61</b>	<b>4.61</b>	<b>3.92</b>	<b>-8.53</b>	<b>3.90</b>	<b>-4.63</b>
<b>SnO<sub>2</sub>/GCC</b>	<b>16.57</b>	<b>4.65</b>	<b>3.73</b>	<b>-8.38</b>	<b>3.90</b>	<b>-4.48</b>

**Table S2.** The fitted data of TRPL curves.

<b>Sample</b>	<b><math>\tau_1</math> (ns)</b>	<b><math>\tau_2</math> (ns)</b>	<b><math>A_1</math></b>	<b><math>A_2</math></b>	<b><math>\tau_{ave}</math>(ns)</b>
<b>SnO<sub>2</sub>/Perovskite</b>	<b>79.06</b>	<b>1081.57</b>	<b>27.12%</b>	<b>72.88%</b>	<b>809.69</b>
<b>SnO<sub>2</sub>/GCC/Perovskite</b>	<b>56.18</b>	<b>889.96</b>	<b>20.34%</b>	<b>79.66%</b>	<b>719.37</b>



**Table S3.** The photovoltaic parameters of the PSCs prepared with and without GCC modification were measured in the reverse scan (RS) and forward scan (FS).

	<b>Sweep direction</b>	<b><math>V_{oc}</math> (V)</b>	<b><math>J_{sc}</math> (mA cm<sup>-2</sup>)</b>	<b>FF (%)</b>	<b>PCE (%)</b>	<b>Hysteresis index</b>
<b>Control</b>	<b>Reverse</b>	<b>1.13</b>	<b>24.70</b>	<b>81.04</b>	<b>22.69</b>	<b>0.045</b>
	<b>Forward</b>	<b>1.13</b>	<b>24.66</b>	<b>77.65</b>	<b>21.68</b>	
<b>Target</b>	<b>Reverse</b>	<b>1.17</b>	<b>25.59</b>	<b>83.61</b>	<b>25.06</b>	<b>0.024</b>
	<b>Forward</b>	<b>1.16</b>	<b>25.59</b>	<b>82.53</b>	<b>24.41</b>	